Journal of Ceramic Processing Research. Vol. 14, No. 4, pp. 529~534 (2013)

J O U R N A L O F
Ceramic Processing Research

The impact of surface morphology on TiAlN film's properties

Fawad Ali, Beom Su Park and Joon Seop Kwak*
Department of Printed Electronics Engineering, Sunchon National University, Sunchon, Chonnam 540-742, Korea

The influence of the surface morphology of titanium aluminum nitride (TiAlN) films, on the hardness and corrosion behavior, was investigated using atomic force microscopy (AFM), scanning electron microscopy (SEM), nano-indentation and potentiodynamic test. With increasing substrate bias voltage and nitrogen flow rate the originally porous and rough surface morphology of the TiAlN films was transferred into a dense and smooth structure. The root mean square (RMS) roughness of the TiAlN films measured using AFM decreased from 3.6 nm to 2.0 nm as the substrate bias was increased from 25 V to 100 V. The experimental results showed that the corrosion resistance and hardness of the coatings increased with decreasing surface roughness. These increases at high substrate bias and high nitrogen flow rate were attributes to the decrease in atomic distance and the reduction in surface porosity.

Key words: TiAlN, Bias, Nitrogen, Morphology, Roughness, Hardness, Corrosion.

Introduction

The materials used for cutting tools are normally subjected to harsh wearing and corrosive conditions. Thus, good mechanical, thermal, and chemical properties are required at elevated temperatures. For this purpose titanium aluminum nitride (TiAlN) has been developed and has been under active investigation as a promising alternative to binary coating materials such as TiN and TiC for cutting tools because it provides good hardness, and wear and heat resistance [1-4, 25]. One of the advantages of TiAlN coatings is that they form a highly adhesive, dense protective Al_2O_3 film at their surface when heated, which prevents further inward diffusion of oxygen into the coated material.

It has been reported [5-7, 24] that the substrate temperature, bias voltage and nitrogen flow rate gas pressure have a great influence on the texture and grain size of deposited films. Especially, the substrate bias voltage and control of reactive gas are critical for the optimization of films in the reactive to produce nitride coatings, and found that film stresses generally increased with increasing bias voltage but that film delimination occurred at high voltage. In addition, the surface of the films became rougher with increasing bias voltage, but the number and size of voids within the films decreased. On the other hand, Musil et al. [18] have reported contradictory results in which the film surface became smoother with increasing substrate bias voltage. Films produced below negative 200 volts were very rough with development of porous microstructure similar to zone 1 of Thornton's [19] structure zone model. At higher bias voltages, a denser and smoother microstructure similar to the zone T structure developed. On the other hand, Hakansson et al. [9] found that coatings produced below a negative bias of 80 volts had a columnar structure with high intra-grain porosity. Increasing the negative bias voltage above 80 volts resulted in a rapid increase in both the lattice parameter and the width of the major (111) peaks. Most of the reports do not describe the effect of substrate bias on surface morphology change, which has significant effect on the mechanical and corrosion behavior of TiAlN coatings.

Mostly TiAlN coatings are synthesized through reactive physical vapor deposition (PVD) methods such as sputtering [9] and [11] ion plating [5]. Several aspects of TiAlN sputter deposited films have recently been reported [8]. Scanning electron microscopy (SEM) and atomic force microscopy (AFM) are important techniques to study the surface morphology of the films and obtain the average root mean square (RMS) roughness, respectively. However, they have not been used to analyze the effect of nitrogen flow rate as a sputtering parameter. The effects of reactive gas on reactive sputtered binary films, such as TiN, TiC, AlN, Si_3N_4 were studied previously [5-7]. Berg et al, [10] proposed a reactive sputtering model for binary compounds and correlated the deposition rate and film composition with the reactive gas flow rate. Breg et al. demonstrated that the deposition rate drastically decreased up to a critical value of nitrogen flow rate but then no more rapid decrease beyond this critical point.

As represented above, several researchers have

*Corresponding author:
Tel : +82-61-750-3559
Fax: +82-61-750-5260
E-mail: jskwak@sunchon.ac.kr

investigated the effect of reactive gas on the surface morphology and roughness of multi-component films such as TiAlN. Neverthless, no systematic study has yet been conducted on the relation between substrate bias voltage and nitrogen flow rates to surface morphology and its effect on various properties of the deposited films. Therefore the basic purpose of this study is to investigate the effect of substrate bias voltage and nitrogen flow rate on the surface morphology, roughness, hardness and corrosion resistance of RF/DC magnetron sputter TiAlN coatings.

Experimental Details

The reactive magnetron co-sputtering technique, with separate titanium and aluminum targets, was used to produce the titanium aluminum nitride (TiAlN) coatings examined in the present study. The TiAlN coatings were deposited with an arrangement of two slightly unbalanced, independently controlled magnetrons. The TiAlN coatings were deposited on silicon and SKD61 steel samples. The SKD61 substrate was mirror polished. Prior to introduction into the chamber, the Si and SKD61 substrates were ultrasonically cleaned in acetone, methanol and deionized water and were dried by blowing nitrogen gas. A turbo-molecular pump backed by a rotary pump was used to achieve a base pressure of 1.5×10^{-6} Torr before introducing the gas mixtures. Once a high vacuum of at least 1.5×10^{6} Torr was reached, the sample holder was heated and maintained at 10 °C for the deposition. The targets were then sputter cleaned with argon for 10 minutes while the substrates were shielded by shutters over the magnetrons. After the pre-deposition, reactive gas of high purity nitrogen was injected into the deposition chamber to form titanium aluminum nitride. The sputtering was carried out in a gas mixture of Ar and nitrogen (99.999 %). The flow rate of nitrogen and Ar was controlled by a mass flow controller. The nitrogen flow rate was varied between 2 to 10 sccm at steps of 2 sccm, and the Ar flow was kept constant at 25 sccm. The negative substrate bias was varied from 25 V to 125 V at steps of 25 V. The target power of the Al (RF) and Ti (DC) targets was 220 W and 150 W, respectively. The working pressure of Ar and nitrogen was set at 5 mTorr. During deposition the substrate was continuously rotating to give uniform coatings. The deposition times at the different nitrogen flows were varied to ensure a constant coating thickness of 450 nm.

X-ray diffraction (XRD), AFM, nano-indentation and potentiodynamic test tests were used to study the microstructure and morphology of the coatings. The microstructure of the coatings was examined using SEM operated at an accelerating voltage of 8 kV. The surface morphology of the coatings was examined using HITACHI S-4800 SEM. The hardness of the coatings was measured by nano-indenter XP (MPS). The crystallographic properties of the coatings were examined by XRD technique using a PANalytical MPD machine. AFM was used to measure the surface roughness. A total of area 5 × 5 mm was used at a scan rate of 0.7 Hz. A Gamry potentiodynamic test was used to measure the corrosion behavior of the coatings on the SKD61 substrate. Alpha step was used to calculate the thickness of the coatings on a glass substrate. The contact angle was used to find the contact angle and surface energy of the coatings.

Results and Discussion

Effect of substrate bias voltage

The XRD patterns of the TiAlN coatings produced at different substrate bias voltages are shown in Fig. 1. All the XRD peaks could be indexed with a cubic TiN structure in the Fm $\bar{3}$ m space group. At low substrate bias voltage, the (220) and (111) peaks were dominant. As the negative substrate bias was increased from 25 to from 125 volts, the peak intensity of the (111) peak increased and of the (220) peak decreased. The 2θ values of the corresponding peaks were also shifted slightly to lower values, suggesting the possible formation of a coating structure with larger lattice parameters at higher negative bias voltages. This peak

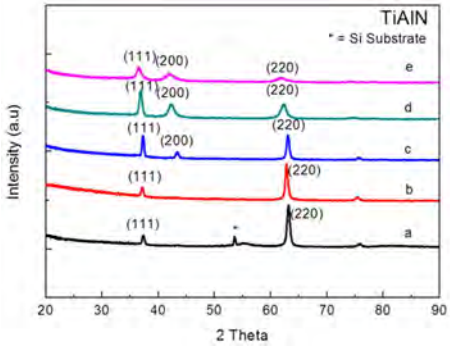

Fig. 1. XRD patterns of the TiAlN coatings produced at different negative bias voltages: 25 V, (b) 50 V, (c) 75 V (d) 100 V and (e) 125 V.

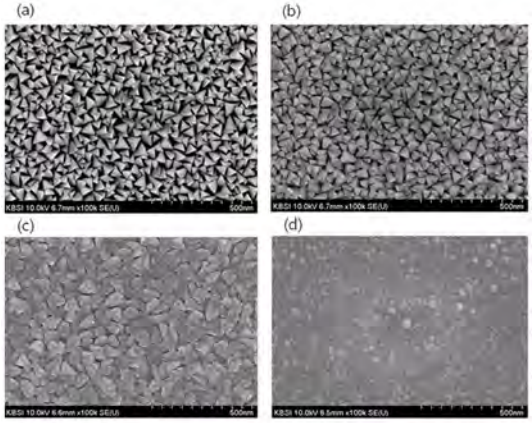

Fig. 2. SEM micrographs of the TiAlN coatings produced at different negative bias voltages:25 V, (b) 50 V, (c) 100 V and (d) 125 V.

broadening and peak shift were attributed to high residual stresses [20, 21]. Fig. 1 also shows that the intensity of the (200) peaks, which was negligible at lower negative bias, increased substantially at the negative bias voltage increased above 75 volts. The emergence of the (200) peak was accompanied by an increase in the film hardness. A similar trend of decreasing (220) peak intensity and increasing (111) peak intensity with increasing substrate bias was also observed by Zywitzki et al. [22] The change in the intensity can be understood in terms of the change in texture of TiAlN with increasing substrate bias voltage. This mechanism is further examined using the SEM micrograph shown in Fig. 2. The increase in substrate bias also produced compressive stresses in the coating and thereby shifted the peak to lower angle.

SEM micrographs illustrating the microstructure and surface morphology of the TiAlN coatings deposited at different substrate bias voltages are shown in Fig. 2. A porous tapered columnar structure similar to the microstructure of zone 1 of Thornton's [19] structure zone model developed at low substrate bias voltage. As the negative bias voltage increased from 75 to 125 volts, the structure became densified, producing a very fine grain structure with features similar to the zone T structure of the Thornton's model. The densified structure can be correlated to the high energy of the depositing atoms at high bias voltage. Although the composition did not change under the different bias voltages investigated, a densified structure with finer grain size and improved surface morphology developed with increasing bias voltage, as shown in Fig. 2.

The RMS roughness measured through AFM decreased from 3.6 nm at a negative substrate bias of 25 volts to 2.0 nm at a negative substrate bias of 125 volts, as shown in Fig. 3. Fig. 2 shows higher magnification views of the surface topography of these coatings. The TiAlN films at low substrate bias (lower than negative bias 100 volts) Figs. 2(a) and 2(b) shows the surface to be faceted, generally terminating in a tetrahedral structure, and with large gaps between them. In contrast, the high substrate biased coatings shown in Fig. 2(c) and 2d have much smaller rounded ends to the surface structures, with no obvious gaps between the structural units which make up the coating. The results shown in Fig. 2 support the previous reports that bias both densifies the coating and reduces the grain size [7]. This apparent increase in the density of the coating with substrate bias has been reported previously by Rickcrby et al. [7] and can be correlated to the surface roughness and hardness of the coatings.

To examine the effect of surface roughness on contact angle, the contact angle was measures. The films deposited at negative substrate biases of 25, 50 and 75 V gave a complete wetting result, while those deposited at 100 and 125 V had an angle of 55.21 and 56.29, respectively. This revealed the rougher and more porous nature of the TiAlN films deposited at low substrate bias voltage.

The coating hardness and Young's modulus were evaluated from nano-indentation test and the results are plotted in Fig. 4. As the negative bias voltage was increased, the coating hardness and Young's modulus increased up to a maximum of 24 GPa (± 4 GPa) at 100 volts. A further increase in the negative bias to 125 volts resulted in a decrease of hardness to 14 GPa. Fig. 3 shows a small increase in hardness up to a negative bias of 50 volts, followed by a steep increase up to 100 volts. The results from Young's modulus evaluation closely replicated the hardness results, as shown in Fig. 4. The Young's modulus increased up to a maximum of 330 GPa at 100 volts with increasing negative bias voltage. An increase in bias voltage has been associated with a change in the stress [26] and structure of the coating, as an increased bias voltage results in a denser, less columnar structure [23]. This postulated change in structure is consistent with the present findings. The increase in substrate bias value enhanced the coating hardness due to the denser microstructure (see Fig. 2).

Effect of nitrogen flow rate

Fig. 5 shows the XRD patterns of the TiAlN coatings prepared at different nitrogen flow rates and with different morphologies. All the XRD peaks could be indexed with a cubic TiN structure in the $Fm\bar{3}$ m space group. As shown in Fig. 5, the coatings showed a

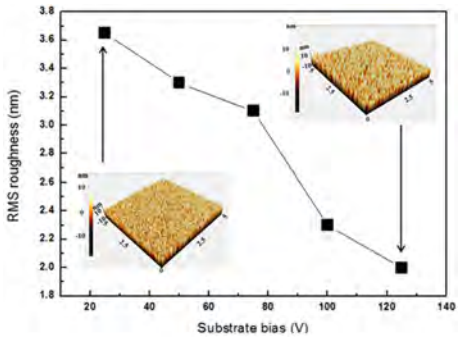

Fig. 3. Surface roughness of the TiAlN coatings as a function of negative bias voltage.

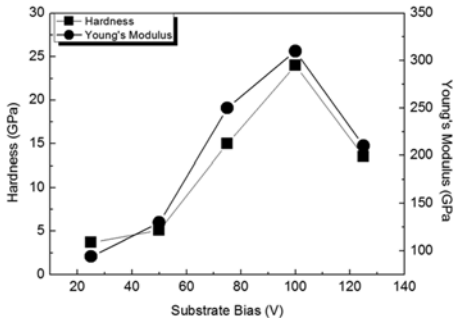

Fig. 4. Hardness and Young's Modulus of the TiAlN coatings as a function of negative substrate bias.

preferred growth along the (220) and (111) directions at a low nitrogen flow rate of 2 and 4 sccm. Weak TiAlN (311) diffraction peaks were also evident. The coating deposited with high nitrogen flow rate (> 6 sccm) exhibited a mixed (111), (200) and (220) TiAlN structure. The (200) peak of TiAlN became clearer at a nitrogen flow rate of 8 sccm. The same trend was also shown by Chen et al. [13] As show in Fig. 5, the (220) peak decreased and the (111) peak increased with increasing nitrogen flow rate. The change in crystal orientation can also be related to the surface morphology, as shown in Fig. 6. When the coatings have a pyramid like structure, then the (220) peak

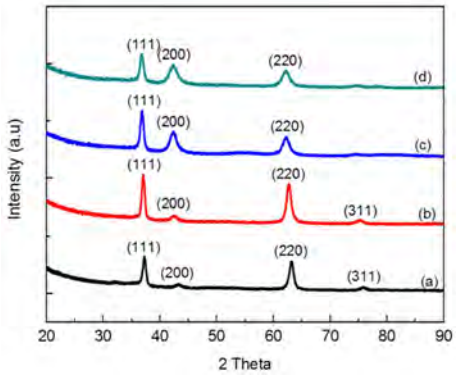

Fig. 5. XRD patterns of the TiAlN coatings produced at different nitrogen flow rates: 2 sccm, (b) 4 sccm, (c) 8 sccm and (d) 10 sccm.

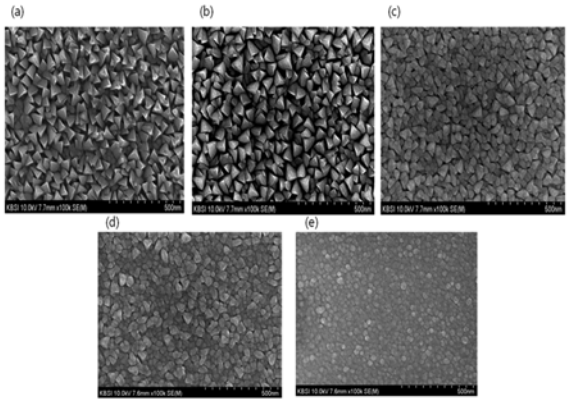

Fig. 6. SEM micrographs of the TiAlN coatings produced at different nitrogen flow rates: (a) 2 sccm, (b) 4 sccm, (c) 6 sccm, (d) 8 sccm and (e) 10 sccm.

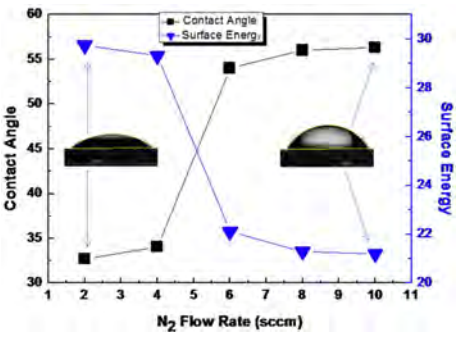

Fig. 7. Effect of nitrogen flow rate on the contact angle and surface energy of the TiAlN coatings.

intensity is high and the surface is more porous. When the surface becomes smoother and denser, the (111) and (200) peaks increase and the (220) peak decreases. Also as shown in Fig. 5, the peak position continually shifted towards lower 2θ values for the main (200) peak with increasing nitrogen flow rate, whereas the shift for the (111) peak was less obvious.

Typical SEM photographs illustrating the surface of the TiA1N films deposited at various N_2 flow rates are shown in Fig. 6. Rough and fractured surfaces were observed in samples reacted at a low N_2 flow rate of 2 sccm, as shown in Fig. 6(a). A mixed crystallized microstructure arose as the N_2 flow exceeded 6 sccm. The grain sizes became finer and the interspacing gradually diminished as the N_2 flow was increased. A dense, isotropic, fine grained microstructure was obtained at a N_2 flow rate of 10 sccm (Fig. 6€). This suggested that the surface of the samples deposited at low nitrogen flow rate consisted of pyramid-like grains separated by pores or voids, as shown in Figs. 6(a) and 6(b), which can be attributed to the preferred growth along the (220) direction of the coatings [13]. The grain sizes became finer and the interspacing gradually diminished as the N_2 flow was increased. Berg et al. [10] also reported a decrease in grain size with increasing nitrogen flow rate. The micro-structural change could be explained as a reduction in atomic mobility with increasing nitrogen flow rate and local variation in the chemical potential on the growing film surface [12].

To examine the effect of surface roughness on the contact angle, contact angle tested was undertaken. The surface energy was measured by a contact angle measurement machine as a function of nitrogen flow rate, as shown in Fig. 7. As observed from the results of the substrate bias, the rougher surface had a higher contact angle than the smoother surface. This indicated that the surface roughness decreased as the nitrogen flow rate was increased, which increased the contact angle and decreased the surface energy. It has been reported [14] that contact angles on rough surfaces are greater than those on relatively smooth surfaces, and that the hysteresis of wetting increases with increasing roughness. Fig. 6 shows that the surface morphology completely changed as the nitrogen flow rate exceeded 4 sccm, and hence that the surface energy and contact angle also changed. At high surface energy, the coatings have low corrosion resistance, and low hardness.

The coating hardness and Young's modulus were evaluated from nano-indentation test and the results are plotted in Fig. 8. The possible influence from the substrate was neglected by keeping the indentation depth to one tenth of the total thickness. Each data point represents an average of ten measurements. The hardness increased steeply as the nitrogen flow rate was increased from 4 to 8 sccm. The increase in hardness was attributed to the change in surface

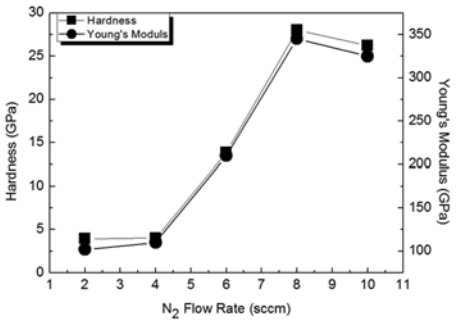

Fig. 8. Hardness and Young's Modulus of the TiAlN coatings as a function of nitrogen flow rate.

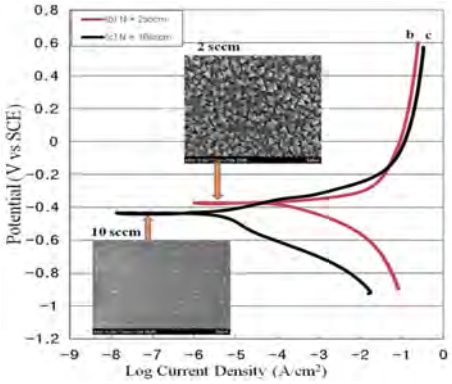

Fig. 9. Effect of surface morphologies on the corrosion resistance of the TiAlN coatings.

morphologies. The smoother surfaces had a higher hardness than the rougher and porous surfaces. The results from the Young's modulus evaluation closely replicated the hardness results, as shown in Fig. 8. The increase in hardness with increasing nitrogen flow rate was attributed to a change in the structure of the coating, such that an increase in nitrogen flow rate resulted in a denser structure and very fine grains, as shown in Fig 6. It is clearly revealed the low hardness of the structures with pyramid-like morphology. When the nitrogen flow rate was increased from 4 sccm, the structure became denser and so the hardness increased. As shown in Fig. 8, the coating hardness and Young's modulus increased as the nitrogen flow rate was increased from 2 to 8 sccm, and then remained nearly constant up to 10 sccm.

In this study, a corrosion test was carried out by immersion test in 1 M HCl electrolyte. The corrosive media of the HCl solutions were adopted for simulating the aggressive aqueous environment containing Cl ions. In the polarization measurement, the corrosion current (Icorr) obtained from the polarization curve was used to evaluate the corrosion resistance of the materials. The uncoated and coated specimens were placed in a Gamry apparatus using corrosive media of 1 M HCl solution. A standard saturated calomel electrode (SCE) was used as a reference and platinum as a counter or auxiliary electrode. The scanning area was 1 cm^2 at a scanning speed of 1 mV/sec.

After polarization test in 1 M HCl solution at room temperature, the polarization curves of the coated SKD61 specimens at a nitrogen flow rate of 2 and 10 sccm were obtained and are shown in Fig. 9. Icorr was calculated by using the Tafel equation. The results showed that the corrosion resistance of SKD61coated samples in 1 M HCl solution was remarkably improved due to improved surface of the TiAlN coatings at the high nitrogen flow rate. In particular, the TiAlN specimens coated at 10 sccm had a low surface roughness and predominantly exhibited better corrosion resistance than that of the high surface roughness specimens. The current density of the sample coated at 10 sccm (C) was significantly lower than the current density of sample (B) coated at 2 sccm. The corrosion current of sample C was the lowest of all the samples. The good corrosion performance of sample C was attributed to its denser microstructure and low surface roughness [15]. Highly orous, non-uniform coatings have been reported to accelerate the corrosion processes due to a galvanic coupling between the coating and the substrate [16]. The present results could be attributed to the dense and smooth morphology of the coatings formed with a slow deposition rate at the nitrogen flow rate of 10 sccm. Hydrophobic surfaces and those with higher contact angle or low surface energy have previously been shown to have greater corrosion resistance [17]. The remarkably large contact angle for sample C, which was close to 60 º compared to 33 º for sample B, indicated that sample C was more hydrophobic than sample B, as shown in Fig. 7. A hydrophobic surface is known to have a lower surface energy than a hydrophilic surface. Combined with the electrochemical results, we conclude that the hydrophobic surface with lower surface energy was correlated to the higher corrosion resistance. This suggests that generically, improved PVD coatings for greater corrosion protection can be developed by reducing the surface roughness and porosity.

Summary

Research was conducted on the effect of substrate bias voltage and nitrogen flow rate on the surface morphology, and the resulting effect on the roughness, contact angle, hardness and corrosion resistance of magnetron co-sputtered TiAlN coatings. As the substrate bias voltage and nitrogen flow rate were increased, the coating structure was densified with the development of a fine grain size, which substantially increased the coating hardness, corrosion resistance, and contact angle and reduced the RMS roughness and surface energy. As observed, the surface morphology strongly influenced the hardness and corrosion resistance of the TiAlN films. The hardness and corrosion resistance of the TiAlN films increased with the decrease of the RMS roughness. The aqueous corrosion protection of

the samples was reduced by the pores and greater roughness that allowed the solution to reach the substrate. However, it was also shown that even a thin but dense coating, such as curve C, could improve the corrosion properties markedly. The deposition rate also varied greatly with the nitrogen flow rate. As the surface morphology became smoother, the corrosion resistance and hardness increased. Overall, the substrate bias voltage and nitrogen flow rate affected the surface morphology of the TiAlN films, which in turn affected the roughness and contact angle, and hence the hardness and corrosion resistance of the coatings.

Acknowledgments

This work was supported by the BK21 PLUS at SCNU and by the Center for Practical Use of Rare Materials, RIC funded by MKE (B0010622).

References

1. K.H. Habig, G.M.Z. Kocker, Surf. Coat. Technol. 62 (1993) 428-437.
2. W. Konig, R. Fritsch, D. Kammermeier, Surf. Coat. Technol. 49 (1991) 316-324.
3. D. Hofmann, B. Hensel, M. Yasuoka, N. Kato, Surf. Coat. Technol. 61 (1993) 326-330.
4. J.M. Molarius, A.S. Korhonen, E. Harju, R. Lappalainen, Surf. Coat. Technol. 33 (1987) 117-132.
5. J.-E. Sundgren, B.-O. Johansson and S.-E. Karlsson, Thin Solid Films. 105 (1983) 383-393.
6. A, J. Perry. M. heRef, W.D. Sproul and P.J. RUdnik, Surf.and Coat. Technol. 42 (1990) 49-68.
7. D.S. Rickcrby and P,J. Burnell. Thin Solid Films. 157 (1988) 195-222.
8. O. Knotek, W.D. Munz, T. Leyendecker, J. Vac. Sci. Technol. A5 (1987) 2173-2179.
9. G. Hakasson, J.-E. Sundgren, Thin Solid Films. 153 (1987) 55-65.
10. S. Berg, H,-O. Blorn,T. Larssonand C, Nender,J. Vac. Sci. Technol. A5 [2] (1987) 202-207.
11. H.A. Jehn, S. Hofmann, V.-E. Ruckborn, W.D. Munz, J. Vac. Sci. Technol. A4 [6] (1986) 2701-2705.
12. B.Y. Shew, J.-L. Huang, Surf. and Coat. Technol. 71 (1995) 30-36.
13. J.T. Chen, J. Wang, F. Zhang, G.A. Zhang, X.Y. Fan, Z.G. Wu, P.X. Yan, Journal of Alloys and Compounds. 472 (2009) 91-96.
14. Bikermani, J. Surface Chemistry for Industrial Research 332. Academic Press, New York. (1918).
15. L. Cunha, M. Andritschky, L. Rebouta, K. Pischow, Surf. and Coat. Technol. 116-119 (1999) 1152-1160.
16. S. Rudenja, C. Leygraf, J. Pan, P. Kulu, E. Talimets, V. Mikli, Surf. and coat. Technol. 114 (1999) 129-136.
17. S. L. Rodhe, W. D. SproulL and J. R. Rodhe, J. Vac. Sci. Technol. A9 (1991) 1178-1183.
18. J. Musil, V. Poulek, V. Valvoda, R. JR. Kuizel, H. A. Jehn and M. E, Baumgartner Surf. Coat. Technol. 60 (1993) 484-489.
19. J. A. Thornton, J. Vac. Sci. Technol. 11 (1974) 666-670.
20. M. Dudek, O. Zabeida, J.E. Klemberg-Sapieha, L. Martinu. J. of Achievements in Materials and Manufacturing Engineering. 37 (2009) 416-421.
21. R. Wuhrer, W. Y. Yeung, Journal of Materials Science. 37 (2002) 1993-2004.
22. O. Zywitzki H. Klostermann, F. Fietzke, T. Modes, Surf. Coating. Technol. 200 (2006) 6522-6526.
23. Y. Tanaka, T.M. Gur, M. Kelly and S.B. Hagstrom, T. Ikeda, Thin Solid Films. 228 (1993) 238-241.
24. S.M. Ha, M.H. Park and S.H. Kim, Journal of Ceramic Processing Research. 13 [S1] (2012) s16-s21.
25. B.W. Lee, D.W. Kim, J.W. Choi, K.H. Bang, G.H. Lee and H. Cho, Journal of Ceramic Processing Research. 9 [6] (2008) 672-677,
26. M.S. Kang, T. Zhang, D.W. Shin, Q. Wang and K.H. Kim, Journal of Ceramic Processing Research. 13 [S1] (2012) s52-s58.